Mid-infrared LEDs versus thermal emitters in IR dynamic scene simulation devices

V. Malyutenko[a], A. Zinovchuk
Lashkaryov Institute of Semiconductor Physics, Kiev, Ukraine

ABSTRACT

In a radical departure from conventional thermal emitter-based dynamic IR scene simulation devices, we have tested InAsSbP/InAs LEDs grown by liquid phase epitaxy and tuned at several peak-emitting wavelengths inside the mid-IR band. Light uniformity, radiation apparent temperature (T_a), thermal resistance, and self heating details were characterized at T=300 K in the microscale by calibrated infrared cameras in the 3-5 μm (light pattern) and 8-12 μm (heat pattern) bands. We show that LEDs are capable of simulating very hot ($T_a \geq 740$ K) targets as well as cold objects and low observable with respect to a particular background. We resume that cost effective LEDs enable a platform for photonic scene projection devices able to compete with thermal microemitter MEMS technology in testing and stimulating very high-speed infrared sensors used for military and commercial applications. Proposals on how to further increase LEDs performance are given.

Key words: 3-5 um LEDs, IR synthetic scene, cold objects, low observable, multispectral testing.

1. INTRODUCTION

The world of infrared (IR) emitting devices operating in the 3-5 μm wavelength band (mid-wave IR, MWIR) is divided into two camps: thermal emitters and photonic devices, like lasers or light emitting diodes (LEDs). For the last two decades, these devices have been increasingly popular because of possible military and commercial applications, including environment monitoring, sensing of chemical weapons, medical diagnostics, and detector testing. To-date, advanced thermal emitter MEMS technology shows its limitation, it seems unlikely that there will be much improvement on the performance already obtained. As a result, the market of these devices has peaked or plateaued. Contrary, photonic approach is in early stage and much work is still underway. Very recently, photonic devices have attracted a great deal of attention mostly due to efficient diode lasers developed in several laboratories and now available for different wavelengths. While capable of emitting high continuous wave (CW) power [at $\lambda \sim 4$ μm, quantum-cascade lasers emit 160 mW at 298 K and 1.6 W at 78 K (Ref.1), interband cascade lasers at λ=3.3-3.6 μm generate 1.1 W at 78 K (Ref.2)], the main drawback to these devices is cost. Indeed, the nanotechnology and testing of diode lasers are expensive processes resulting in a >10:1 price ratio between lasers and LEDs available in the market. From the other side, there are strong signs that 3-5 μm LEDs are poised for a potential rebirth. Improving device technology and design has enabled to achieve pulse power output well above 1mW at room temperature[3-5]. From the short wavelength side, there are devices based on GaSb and InGaAs heterostructures[6,7]. The InAs ternary and quaternary compounds form a basis for the central part of the MWIR, while InSb and HgCdTe LEDs stay at the long wavelength side[8-12]. Thus, conventional LEDs are becoming feasible emitters for unguided long distance communication, long-base "light barrier" devices, MWIR illuminators, and IR countermeasure technologies. By authors' opinion, the most important application of MWIR LEDs, but one, which is rarely mentioned[13,14], is that of dynamic infrared scene projection (DISP) devices. There are several reasons for market demand for these devices - high operation speed imaging (> 20 kHz frame rate), multispectral imaging (several sub-bands inside the mid-infrared atmospheric transparency window), and negative-temperature background simulation **(**like winter or arctic scenes, and space background). Advanced MEMS-based IR scene simulators composed of thermal IR emitters satisfy none of these options.

In this letter, we examine whether conventional LEDs can form a platform for photonic MWIR DISP devices able to compete with advanced thermal microemitter technology[15,16] in testing and stimulating IR sensors, including forward-looking IR missile warning systems, IR search-and-track devices, and missile seekers. We also consider how they relate to the laser-based DISP technology which also worth to be mention even if not commercially realized yet. We

[a] E-mail: malyut@isp.kiev.ua

Optoelectronic Devices: Physics, Fabrication and Application III, edited by Joachim Piprek, Jian Jim Wang. Proc of SPIE Vol. 6368 (SPIE, Bellingham, WA, 2006) –0277-786X/ 05/ $15 – doi: 10.1117/12.686830

show that the IR LEDs have the potential to develop new generation of DISP devices capable of simulating not only hot point or extended targets (what thermal emitters or lasers can) but cold objects and low observables[17] (what their counterparts can't by the definition) as well. We experimentally demonstrate that high performance can be obtained from LEDs grown by liquid phase epitaxy (LPE) process which owing to its simplicity and low cost has been used for fabricating heterostructures since the middle 1960s.

2. EXPERIMENTS

Our study is primary concerned with testing the InAsSbP devices. To demonstrate the availability and accessibility of the approach, the devices under test were obtained from industrial manufacturers. The LED active regions examined here are grown on ~200 μm-thick InAs substrates by LPE as InAsSbP/InAsSb double heterostructures. These structures benefit is that the peak-emitting wavelength (λ_p) can be tailored over the MWIR by merely changing the Sb content in the InAsSb active layer. The chips were packaged into TO-39 case as substrate-down planar (450 x 450 μm^2) or substrate-up circular (D=300 μm) mesa structures and designed as single elements or 4 x 4 diode bars operated in forward (electroluminescence) and reverse (negative luminescence[17]) bias modes.

In a planar structure, the top opaque metal contact (d=100 μm) prevented some of the light from passing through the front emitting surface, reducing the optical efficiency and power output. And contrary, the emitting area of a mesa structure was free of contacts as both electrodes were formed on the opposite side of a chip with a 150 -μm-diameter central contact (Fig.1). The points of interest were the uniformity of light and heat in microscale in devices of different geometrical form and the local structure overheating that limits CW operation at room temperature. Also we wanted to see how the current crowding (CC) effect that prevents LED from being made very large area[18] depends on the emitting wavelength. However, our major goal was to measure the apparent temperature (T_a) of radiation emitted by LEDs tuned at different λ_p (T_a is determined as the temperature of a black body of equal power emitted in the spectral range of interest).

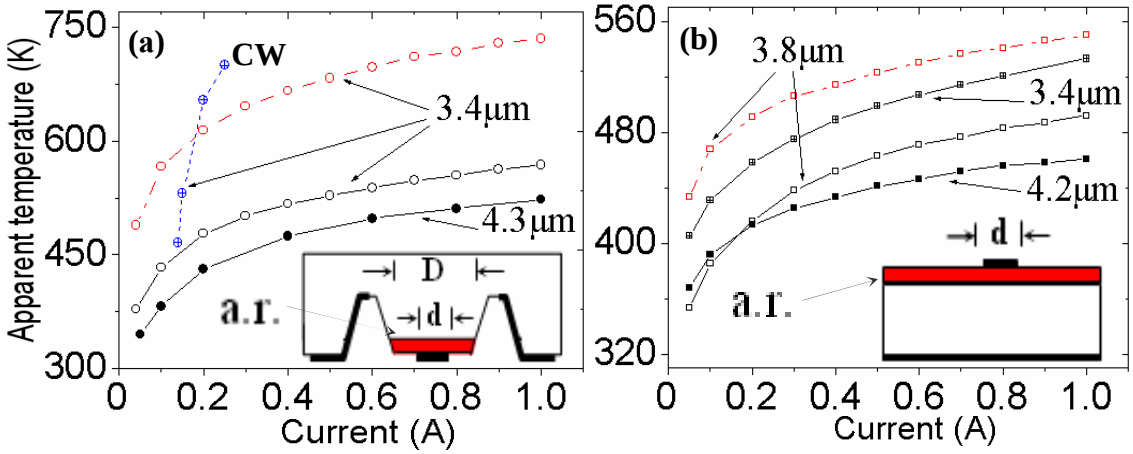

Fig.1.Measured apparent temperature T_a as a function of bias current for mesa (a) and planar (b) LEDs tuned at different λ_p. Dashed lines show narrow-band tests with filter passband $\Delta\lambda/\lambda_p$= 8.0 and 10.5 % for λ_p=3.4 and 3.8 μm respectively. Solid lines relate to MWIR-band tests. CW curve mesured at T=200 K. The insets are schematics of mesa and planar structures with active region (a. r.) shown in red.

The light pattern, heat distribution, and T_a values were characterized by the test system consisting of IR scanning cameras operating in 3-5 μm (IR light mapping) and 8-12 μm (heat mapping) bands in a pulse slave mode (50 μs -160 ms pulse duration) with radiometric and thermographic calibration. When equipped with the IR microscope, these cameras enable the < 20 μm spatial resolution (10 μm scanning step), the temperature resolution of ~ 0.1^0 C, and the 10 μs time-resolved interval. As the LED spectra are not broadband like a blackbody used for calibration and camera spectral response is not usually flat, the T_a measurements with calibrated narrow-bandpass filters matched to spectra of LEDs were also performed. The filter band was taken equal half-width-at-half-maximum ($\Delta\lambda$) of LED spectrum. It is due to specificity of the thermographic calibration that for users of photonic DISP devices both these parameters (MWIR-band T_a and narrow-band T_a) are of interest.

3. RESULTS AND DISCUSSION

Figure 1 shows apparent temperature (far-field view) versus current (T_a-I) characteristics for mesa and planar LEDs tuned at different λ_p and maintained at T~300 K (but not the CW curve). As the spatial distribution of light was not uniform across the emitting surface (see Fig.2), only "brightest" regions were selected to measure T_a. To minimize an active area overheating, tests were recorded at current pulse length

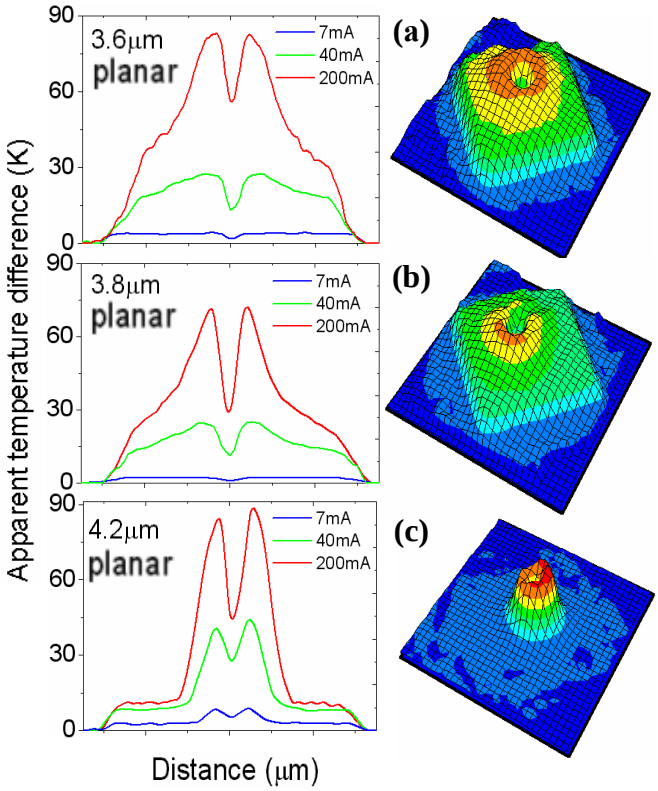

Fig.2. Left column: the ΔT_a profiles in planar (along the diagonal crossing) LEDs at different bias currents. Right column: the ΔT_a spatial view at I=40 mA.

of 50 μs and 25 Hz repetition rate. Careful verification was conducted to ensure that the pulsed IR emission at all current values was predominately of a luminescence nature and not a "thermal" one stemming from the Joule heating and a non-radiative carrier recombination processes. The data show that coming from the short wavelength side of MWIR, apparent temperature of radiation gradually decrease when λ_p increases. This may be due to the Auger recombination impact and because of increase of equilibrium power emitted by longer wavelength-emitting LEDs. Meanwhile, narrow-band T_a values are compared to those (~740 K) achieved by the thermal emitters[15]. To this end, our tests shown that only slightly cooled (T ~ 200 K, the temperature of a conventional Peltier cooler) LEDs are easy to step over this limit in CW mode at I ≥ 200 mA (see CW curve Fig.1a).

The single-line (400 μs pulse duration) profile and two-dimensional distribution (160 ms frame duration) of light on the plane orthogonal to the beam propagation path captured by a microscope focused on the p-n junction area (near-field view) are shown in Fig.2 (planar) and Fig.4 (mesa) at different bias currents. The parameter of interest is the difference between apparent temperature at given current and the background $\Delta T_a = T_a(I) - T_a(0)$. At low current, the light pattern is uniform across both planar and mesa active areas. Increasing current, however, results in a catastrophic decrease of the emitting area in planar structures with top point contact (this contact shadow is clearly seen in all figures). More details are show in Fig.3 where the filling factor (F) of emitting surface (conditionally determined as the part of an active surface where T_a values exceed 80% of the maximum) is plotted against the forward current. It is the CC that makes the emitted

light to concentrate symmetrically around the top contact and "forget" a device geometry[18,19]. Longer the λ_p smaller is the filling factor by decreasing from 10% (λ_p = 3.4 μm) to ~1.5% (λ_p = 4.2 μm). As a result, measured at I = 40 mA CW power outputs in planar structures were 24 μW (3.6 μm), 21 μW (3.8 μm), and 15 μW (4.2 μm).

In mesa structures, CC decreases the emitting area by D^2/d^2 times (F=25%) but this "crowded" light escapes the structure that is free of contact shadowing (Fig.4). Further current increase causes an additional non-uniformity in light distribution: two peaks appear at the edges of a mesa with a maximum in between (see also bright ring in the 2D distribution). These satellites originate from the light laterally escaping a mesa and reflecting from its cone ("internal focusing") and result in ~20% power output increase. This makes mesa structures more efficient source for DISP devices.

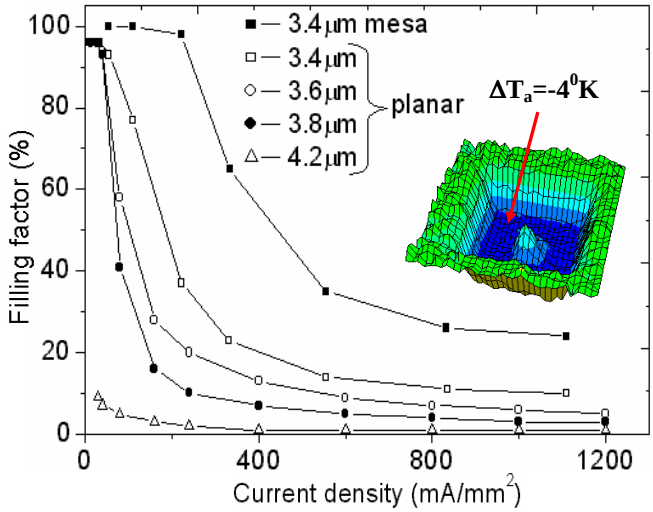

Fig.3. Filling factor as a function of bias current. The inset shows the ΔT_a spatial view over the 3.8 μm planar structure at I= -10 mA (the negative luminescence mode).

Although recombination losses, Joule losses, CC effect, and low thermal conductivity of III-Vs combined contribute to dangerous self-heating of IR LEDs, only a few researches have been focused on the thermal behavior of these devices and attempts to visualize heat pattern with a high degree of clarity[19]. To get more details on LED heat signature, "thermal" signal measurements were performed with the 8-12 μm camera. Heat pattern was clearly seen provided current pulse duration was less than the heat relaxation time. As an example, shown in Fig.4 is the heat trap in a mesa structure registered through the InAs substrate. Due to possible absorption of thermal radiation by a doped substrate, absolute temperature measurements in active area were problematic. However, bell-like temperature distribution clearly indicates the region where current flows.

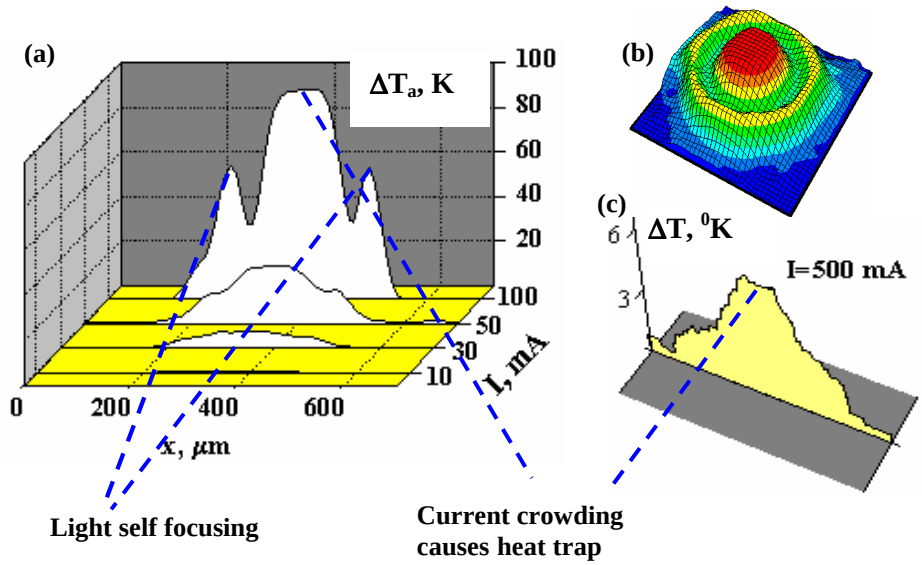

Fig.4. a) The ΔT_a profiles in 3.4-μm-mesa (along the diameter crossing) LED at different bias currents. The vertical scale for the lowest current (I=10 mA) is twice increased. b) The ΔT_a spatial view at I=40 mA. c) One-dimensional heat distribution captured in 8-12 μm band.

The CW tests have shown that the thermal resistance (determined as the slope of linear relationship between the junction temperature and drive power) was ~75 K/W in "bright" 3.4 μm-planar LED, while it increased up to 85 K/W in less efficient 3.8 μm LED. For a comparison, in the 3.4 μm-mesa this value was only 52 K/W that looks like another benefit of mesa structures. The details of junction overheating and heat relaxation time versus electric power are shown in Fig.5. In particular, heat relaxation process measured in a pulsed mode (pulse duration is 3.5 ms) in LWIR band shows that in 3.4, 3.6 and 3.8-μm-LED's thermal constants are 1.8, 2.4, and 4.0 ms respectively. Also important is that the longer LED wavelength the more heat a device generates (compare maximum thermal power pulsed values).

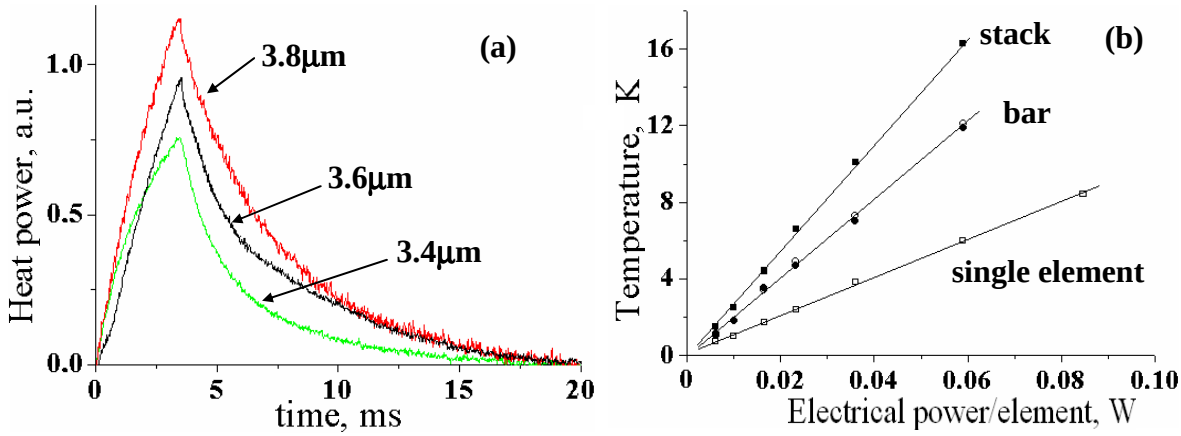

Fig.5. (left) Heat relaxation process measured in pulsed mode. (right) Single LED self-heating measured in a stack of LEDs when single element, 4-element bar, and 4 x 4 stack are "on". The lines are linear fits to the data.

In the negative luminescence mode[17], practically all junction area remains active (see inset in Fig.3 and Fig.6, d). This is due to high junction resistance (in respect to the emitter resistance) that contributes to the current spreading across all active LED region[18]. It is very important that combining forward and reverse bias evidences unique IR LED property- the ability to simulate hot or cold target and low observable with respect to a particular background. Indeed, as real targets effectively reduce their observability features applying Stealth technologies, modern DISP devices must keep up

with new synthetic scenarios through projecting target signatures, which are virtually invisible to IR sensors (real-time active camouflage simulation). Shown in Fig.6 is the experimental CW demonstration of H. Wells's paradox[20] in the MWIR. In the initial state (a, I=0), the circular active region of a 4.3-μm-mesa LED (1) and the rest part of structure (2) are slightly seen due to emissivity difference between these regions (T_a=35^0 C) and Si carrier (3, T_{Si} =33^0 C) on which the structure sits. This positive thermal contrast becomes higher at forward bias (b, I>0); the active region looks "warmer" (T_a=41^0 C). In the negative luminescence mode (I<0), camera detects the active device area as low observable (c, negligible temperature contrast between the object and the background (ΔT~0) or cold object (d, T_a = 30^0 C).

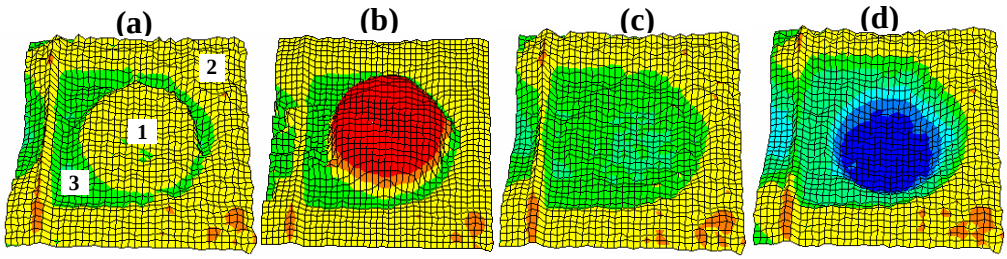

Fig.6. (a) In the initial state, the MWIR camera maps a mesa like an object (1, 2) and a background (3) with positive contrast in between. Positive bias (I= 50 mA) makes the contrast to increase (b, ΔT= 8 K) while negative bias makes the active region difficult to resolve (c, zero contrast, low observable, I= -20 mA) or transforms it in a cold object (d, ΔT=-3 K, I= -50 mA).

Finally, an array of 4 x 4 closely-spaced 3.4-μm LEDs that are independently addressable can be used in simulating separate point sources and extended targets (Fig.7). The advantage of this approach over thermal emitter technology is that multiple emitting wavelengths λ_p can be combined within the array. However, tests show that mutual heating of small-area individual LEDs in an array is controlled by the overlap of local temperature fields in a heat spreader (Fig.5). Indeed, CW thermal resistance of a single emitter was of 90 K/W; this value increased up to 200 K/W in a four-LED bar, and it jumped up to 290 K/W in a stack of bars. This can makes simulating very hot extended targets in CW problematic and demands for more efficient thermal strategy (like, for example, the microchannel heat sink, or Peltier cooler).

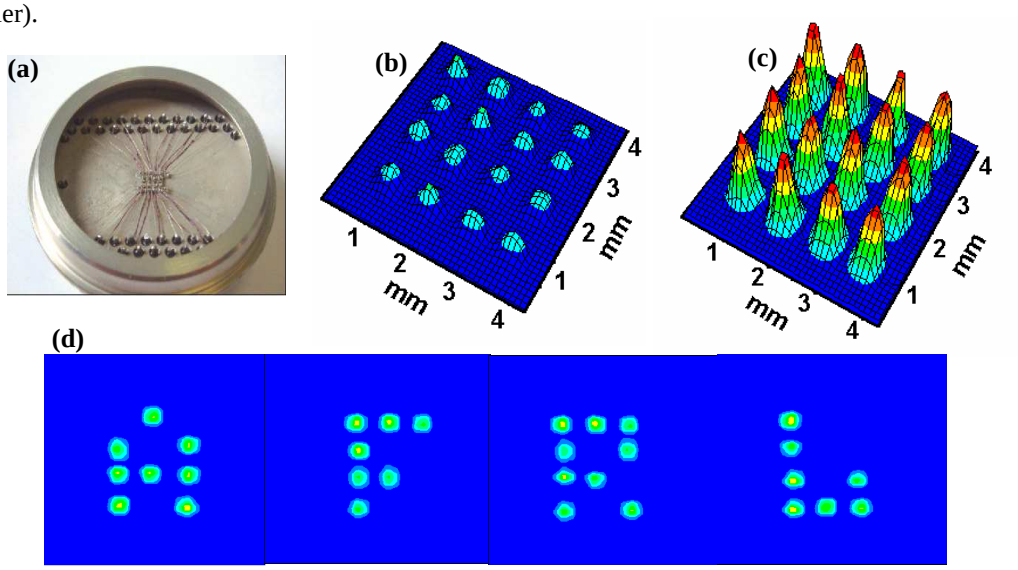

Fig.7. (a) The 4 x 4 hand-made LED array composed of 16 point sources emitting at 3.4 μm. (b, c) The MWIR camera captures a group of point sources, that are connected in shunt and positively biased. The modulated apparent temperatures are ΔT_{max}=25 and 95 K at I=50 (b) and 600 mA (c) respectively. (d) It takes only 50 mA to reproduce our partner's "positive" brand.

4. CONCLUSION

In summary, it has been demonstrated that the 3-5 μm LEDs fabricated entirely in a single LPE run (a process suitable for mass production) as substrate-up mesa structures can form ideal platform for new generation of photonic DISP devices operating at room temperature with relatively high spectral output density. Indeed, these devices have much to offer in nearly every aspect of DISP application. Still in early stage and far from optimum, they allow high-speed (>20 KHz) simulating high apparent temperature (T_a ~750 K, thermal emitter limit) targets even if the structures and design are not fully optimized for DISP purposes. Being neither monochromatic like a laser nor broadband like a blackbody, LEDs can become the heart of multi-spectral narrow-band DISP devices operating inside the MWIR band. For this application, IR LEDs are better than diode lasers because of their superior stability, less directional nature of light emitted, and lower cost. (However, LEDs cannot compete with lasers in the hyper-spectral DISP technology). But the major advantage of this approach that could have a very large impact is in ability to simulate dynamically cold scenes (even though a device sits at room temperature) and low observable. Note there is no problem in high-speed maintaining this chameleon effect even if the background temperature is not stable. These futures can revolutionise the DISP technology.

Although these power hungry off-the-shelf devices exhibit very low external efficiency and suffer from excessive self-heating, they already are very strong contenders in the DISP market. We expect that the surface patterning, large-area reflective bottom contact, intended mesa sidewall profiling (more efficient light extraction), current spreading, lower barrier and contact resistance (lower power consumption), and packaging technology with lower thermal resistance (better heat sink) can lead to an up twofold T_a increase in CW mode. Clearly we think the long-rage future of the photonic DISP technology is strong and the results presented can provide starting point for further device and technology improvements.

ACKNOWLEDGEMENT

We gratefully acknowledge financial support by the Air Force Research Laboratory. We also express our heartfelt thank to Dr. Robert Lee Murrer (formerly at AFRL) for initiating this work and O. Malyutenko for help in measurements.

REFERENCES

1. J. S. Yu, S. R. Darvish, A. Evans, J. Nguyen, S. Slivken, and M. Razeghi, “Room-temperature continuous-wave operation of quantum cascade lasers at λ~4 μm”, Appl. Phys. Lett. **88**, 041111, (2006).
2. C. L. Canedy, W. W. Bewley, J. R. Lindle, C. S. Kim, M. Kim, I. Vurgaftman, and J. R. Meyer, “High-power and high-efficiency midwave-infrared interband cascade lasers”, Appl. Phys. Lett. **88**, 161103, (2006).
3. V. V. Sherstnev, A. M. Monakhov, A. Krier, and G. Hill, “Superluminescence in InAsSb circular-ring-mode light-emitting diodes for CO gas detection”, Appl. Phys. Lett. **77**, 3908-3910, (2000).
4. B. A. Matveev, N. V. Zotova, N .D. Il’inskaya, S. A. Karandashev, M. A. Remennyi, N. M. Stus’, and G. N. Talalakin, “Towards efficient mid-IR LED operation: optical pumping, extraction or injection of carriers?“, J. Mod. Optics **49**, 743-756, (2002).
5. B. Zhurtanov, É. V. Ivanov, A. N. Imenkov, N. M. Kolchanova, A. E. Rozov, N. Stoyanov, and Yu. P. Yakovlev, “High-efficiency 3.4-4.4 μm light-emitting diodes based on a p-AlGaAsSb/n-InGaAsSb/n-AlGaAsSb heterostructures operating at room temperature“,Technical Physics Letters **27**, 173-175, (2001).
6. A. N. Imenkov, E. A. Grebenshchikova, B. E. Zhurtanov, T. N. Danilova, M. A. Sipovskaya, N. V. Vlasenko, Yu. P. Yakovlev, “Properties of GaSb-based LEDs with grid ohmic contacts”, Semiconductors **38**, 1356-1363, (2004).
7. B. A. Matveev, M. A. Aydaraliev, N. V. Zotova, S. A. Karandashov, N. D. Il’inskaya, M. A. Remennyi, N. M. Stus, G. N. Talalakin, “Flip-chip bonded InAsSbP and InGaAs LEDs and detectors for the 3-μm spectral region”, IEE Proc. Optoelectronics, **150**, 356-359, (2003).
8. W. W. Bewley, J. R. Lindle, I. Vurgaftman, and J. R. Meyer, “Negative luminescence with 93% efficiency from midwave infrared HgCdTe diode arrays”, Appl. Phys. Lett. **83**, 3254-3256, (2003).
9. T. Ashley, C. T. Elliott, N. T. Gordon, R. S. Hall, A. D. Johnson, and G. J. Price, “Uncooled InSb/$In_{1-x}Al_xSb$ mid-infrared emitter”, Appl. Phys. Lett. **64**, 2433-2435, (1994).

10. V. K. Malyutenko, S. S. Bolgov, and O. Yu. Malyutenko," Multielement IR Sourses with Alternative Contrast", Techn. Phys. Lett**. 27**, 644-646, (2001)
11. V. K. Malyutenko, S. S. Bolgov, O. Yu. Malyutenko, "Two-dimensional InSb array of IR emitters with alternating contrast", Infrared Phys. Technol. **44**, 11-15, (2003).
12. M. K. Haigh, G. R. Nash, N. T. Gordon, J. Edwards, A. Graham, J. Giess, J. E. Hails, and M. Houlton, "Long wavelength HgCdTe on Si negative luminescence devices", Appl. Phys. Lett. **86**, 011910, (2005).
13. V. Malyutenko, O. Malyutenko, A. Zinovchuk, N. Zotova, S. Karandashev, B. Matveev, M. Remennyi, N.Stus, "InAs(Sb) LEDs and negative luminescence devices for dynamic scene simulation in the first atmospheric window (3-5 μm)", 6th Int. Conf. on Mid-Infrared Optoelectronics Material and Devices, St. Petersburg, Russia, 28 June-2July 2004, Book of Abstracts, pp. 77-78.
14. Naresh C. Das, Kim Olver, F. Towner, G. Simonis, and H. Shen, Appl. Phys. Lett. "Infrared (3.8 μm) interband cascade light-emitting diode array with record high efficiency", **87**, 041105, (2005).
15. D. Brett Beasley, Daniel A. Saylor, and Jim Buford, "Overview of dynamic scene projectors at the US Army Aviation and Missile Command", Proc. SPIE **4717**, 136-147, (2002).
16. Paul Bryant, Jim Oleson, Jay James, Steve McHugh, John Lannon, David Vellenga, Scott Goodwin, Alan Huffman, Steve Solomon, George C. Goldsmith II, "MIRAGE: developments in IRSP systems, RIIC design, emitter fabrication, and performance", Pros. SPIE **5785,** 1-13, (2005).
17. V. Malyutenko, "Negative luminescence in semiconductors: a retrospective view", Physica E: Low-dimensional Systems and Nanostructures **20**, 553, (2004).
18. V. K. Malyutenko, O.Yu. Malyutenko, A. D. Podoltsev, I.N. Kucheryavaya, B. A. Matveev, M. A Remennyi, and N. M. Stus, "Current crowding in InAsSb light emitting diodes", Appl. Phys. Lett. **79**, 4228, (2001).
19. V. Malyutenko, O. Malyutenko, A. Dazzi, N. Gross, and J-M. Ortega, "Heat transfer mapping in 3-5 μm light emitting structures", J. Appl. Phys. **93,** 9398, (2003).
20. H.Wells, "The Invisible man", (1897).